

July 13, 2023

Towards an integrated determination of proton, deuteron and nuclear PDFs

TANJONA R. RABEMANANJARA

*Department of Physics and Astronomy, Vrije Universiteit, NL-1081 HV Amsterdam
Nikhef Theory Group, Science Park 105, 1098 XG Amsterdam, The Netherlands*

We present progress towards a unified framework enabling the simultaneous determination of the parton distribution functions (PDFs) of the proton, deuteron, and nuclei up to lead (^{208}Pb). Our approach is based on the integration of the fitting framework underlying the nNNPDF3.0 determination of nuclear PDFs into that adopted for the NNPDF4.0 global analysis of proton PDFs. Our work paves the way toward a full integrated global analysis of non-perturbative QCD – a key ingredient for the exploitation of the scientific potential of present and future nuclear and particle physics facilities such as the Electron-Ion Collider (EIC).

PRESENTED AT

DIS2023: XXX International Workshop on Deep-Inelastic
Scattering and Related Subjects,
Michigan State University, USA, 27-31 March 2023



Introduction. Future measurements at the recently approved Electron-Ion Collider (EIC) [1,2] and at the High-Luminosity Large Hadron Collider (HL-LHC) [3] will perform key measurements that can pin down the dynamics of Quantum Chromodynamics (QCD). By colliding (polarized) beams with proton or deuteron or heavier nuclei for a range of center-of-mass energies, these experiments will be fundamental in understanding how partons are distributed in momentum and position spaces within a proton and how the parton distribution of nucleon bound within nuclei are modified w.r.t. their free-nucleon counterparts.

In order to fully interpret the precision-level measurements offered by such experiments, the theoretical determination of both the unpolarized proton and nuclear parton distribution functions, henceforth referred to as (n)PDFs, needs to be improved. While the determination of the free-proton PDFs has seen quite an advancement in recent years [4] – owing mostly to the availability of a broad experimental dataset and theoretical improvements in higher-order calculations – the current status in the determination of nuclear PDFs is somewhat less advanced. In addition, albeit both proton and nuclear PDFs are simultaneously constrained by datasets where one of the targets or projectiles is not a free-state proton, their extractions are usually performed in a separate manner.

On one hand, it has been well understood that measurements involving deuteron and heavier nuclear targets play a significant role in disentangling the proton’s quark and antiquark distributions, and in separating the up and down PDFs for large momentum fractions in which searches for physics beyond the Standard Model (BSM) are relevant [5]. In the past, different approaches have been adopted to account for nuclear corrections in proton PDF fits, each with its own motivations and limitations. The approach adopted in the NNPDF methodology [6,7] consists in adding the uncertainties due to nuclear effects as an extra contribution to the theory covariance matrix [8–10].

On the other hand, all hadronic datasets included in the determination of nuclear PDFs involve a free-proton in the initial state. Most nuclear PDF sets are therefore determined assuming a fixed proton baseline which can be considered as a theoretical bias whose effect is difficult to estimate. In the nNNPDF methodology [11–13], although the $A = 1$ dependence (with A representing the atomic mass number) is also fitted in the same footing as $A \neq 1$ by means of a neural network, a fixed proton baseline is still required to enforce the $A \rightarrow 1$ limit, therefore introducing a potential bias in that the back-reaction of the fitted data on the proton PDF is ignored. Such a constraint is imposed at the level of the χ^2 as a penalty by means of a Lagrange multiplier.

Motivated by the need for a consistent and concurrent extractions of the unpolarized proton, deuteron, and heavier nuclear PDFs, we present here work in progress towards an “integrated fit” (see also [14] for a first attempt) in which the atomic mass number dependence is smoothly parametrized from $A = 1$ to $A = 208$ by fitting simultaneously to proton, deuteron, and heavier nuclear datasets, removing the need for imposing a boundary condition for the $A = 1$ limit. A similar idea was applied to PDFs and fragmentation functions by the JAM collaboration in [4,15]. Our approach is based on the integration of the fitting framework underlying the nNNPDF3.0 determination of nuclear PDFs into that adopted for the NNPDF4.0 global analysis of proton PDFs [7]. As a first attempt to apply our methodology, we perform fits in which only deep inelastic scattering (DIS) processes are included using NNLO QCD calculations with perturbative charm.

Here we briefly describe the integrated fitting framework, emphasizing on the its main differences w.r.t the (n)NNPDF approaches. We then study the stability of the integrated fits based on the NNPDF4.0 default hyperparameters from which all the subsequent results are derived. We assess the impacts of the integrated fitting methodology on the proton and nuclear PDFs by comparing the results with the reference (n)NNPDF determination. Conclusions are drawn in the last section.

Methodology. As mentioned above, the integrated fitting methodology incorporates the nuclear PDF parametrization from nNNPDF3.0 into the determination of free-proton PDF using the NNPDF4.0 methodology. The reason for this is twofold. First, albeit the nNNPDF3.0 is also based on deterministic minimization algorithm it does not provide some of the advanced machine learning techniques that the NNPDF4.0 possesses – such as the automatic tuning of the hyperparameters using the k -folding procedure [6,7]. In addition, the NNPDF4.0 methodology also provides ways to carefully validate the resulting PDF uncertainties via the closure and future test approaches. Nonetheless, the two determinations share a large number of similarities, one among which is the parametrization of the (n)PDFs in the evolution basis.

The main modification to the NNPDF4.0 methodology to account for the nuclear fit consists in parametrizing the A -dependence of the (n)PDFs during the fit. That is, the relation between the output of the neural network and the (n)PDFs is given by:

$$x f_k^A(x, Q_0; \theta) = \eta_k^A x^{1-\alpha_k^A} (1-x)^{\beta_k^A} \text{NN}_k^A(x, Q_0; \theta), \quad (1)$$

where k runs over the elements of the PDF in the evolution basis, $\text{NN}_k^A(x; \theta)$ is the k -th output of the neural network, θ indicates the full set of neural network parameters, η_k^A is the normalization corresponding to the k -th PDF, and A represents the atomic mass number of the proton/deuteron/nucleus. Note that in principle the preprocessing exponents α_k^A and β_k^A should also depend on A . The way in which such a dependence on the atomic mass number A is propagated through the fitting framework is illustrated in Fig. 1.

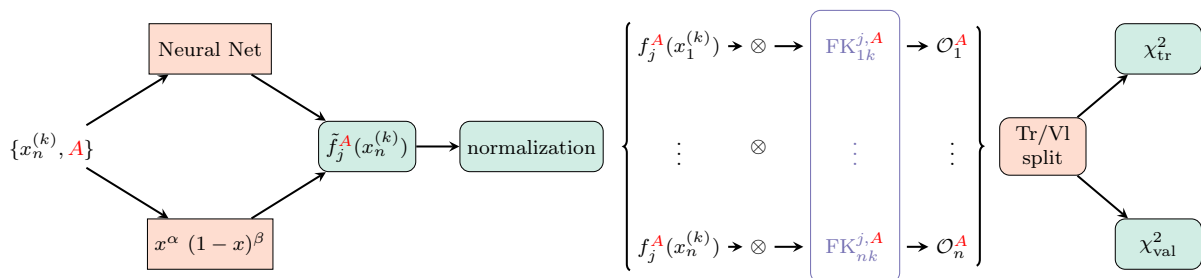


Figure 1: A modified version of Fig. 3.2 from [6] with the additional A -dependence.

In order to test the integrated framework, we focus in the present study on fits to DIS datasets only which include measurements on proton, deuteron, and nuclear targets as comprised in the (n)NNPDF determinations. As theory inputs, we use NNLO QCD calculations provided by the new theory pipeline used in the NNPDF framework [16]. And in order to be able to compare to previous nNNPDF PDF releases, we take the approach in which charm is generated perturbatively. The fitting scale and the kinematic cuts are taken to be the same as in the default NNPDF4.0 methodology, refer to [6,7] for more details.

Training stability. The baseline hyperparameters used in the present analysis for the integrated fit are the same as the ones used in the default NNPDF4.0 methodology extracted from a k -folding hyperoptimization procedure. These are listed in Table 3.7 of [6] with the difference that now the maximum number of epochs is larger to account for the longer training. Owing to the more complex two-dimensional parameter space (x, A) to be fitted [17] – as opposed to the one-dimensional space relevant for a free-proton PDF determination in which only the x -dependence is parametrized – one indeed expects the integrated fit to converge slower.

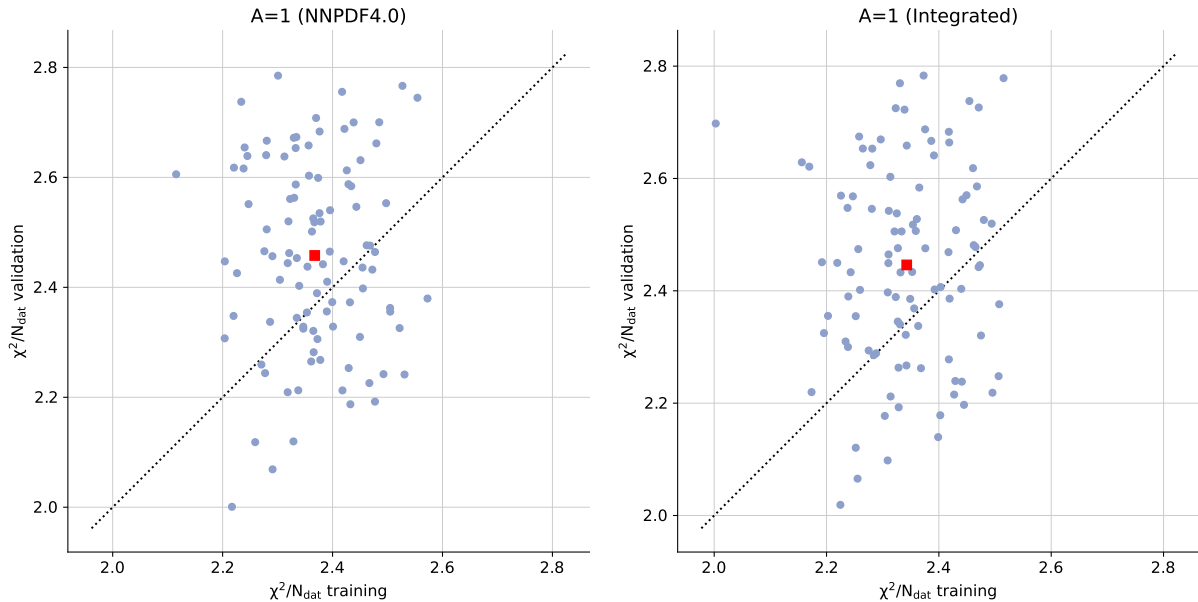


Figure 2: Distribution of the training χ^2 values over the different replicas for the default NNP4.0 (left) and integrated methodologies (right). The red square represents the mean value over the replicas.

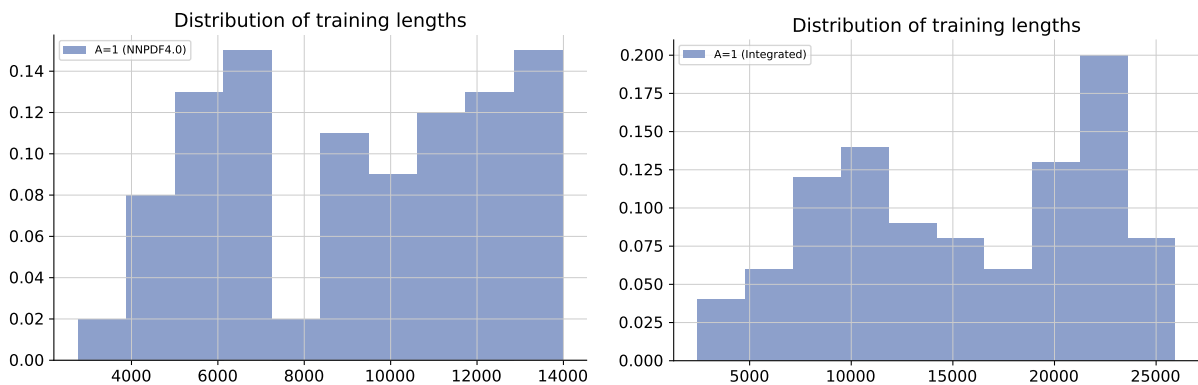


Figure 3: Distribution of the training lengths over the replicas that passed the postfit selection criteria for the default NNP4.0 (left) and integrated methodologies (right).

Table 1 compares the fit quality between a free-proton fit determined using the default NNP4.0 methodology and a combined proton and nuclear fit determined using the integrated framework. Displayed are the total experimental χ^2_{exp} per data point for all the datasets entering each determination, the average experimental $\langle\chi^2_{\text{exp}}\rangle$ over the replica, and the experimental training and validation error functions $\langle E_{\text{tr}}\rangle$ and $\langle E_{\text{val}}\rangle$.

Methodology	χ^2_{exp}	N_{dat}	$\langle\chi^2_{\text{exp}}\rangle$	$\langle E_{\text{tr}}\rangle$	$\langle E_{\text{val}}\rangle$	Tr. Lengths
NNP4.0	1.291	1788	1.336 ± 0.028	2.328 ± 0.087	2.440 ± 0.180	9200 ± 3200
Integrated	1.322	3161	1.357 ± 0.030	2.360 ± 0.088	2.460 ± 0.170	15700 ± 6400

Table 1: Comparison of the fit quality between the free-proton only and integrated fits.

From Table 1 one finds that in the integrated fit a good description of the experimental data which includes nuclear datasets is achieved, with a total of $\chi^2_{\text{exp}} = 1.322$ per data point. Looking at the χ^2 -breakdown we see that the total experimental $\chi^2_{\text{exp}}(A = 1) = 1.192$ on the proton datasets is much smaller than the value obtained from the free-proton

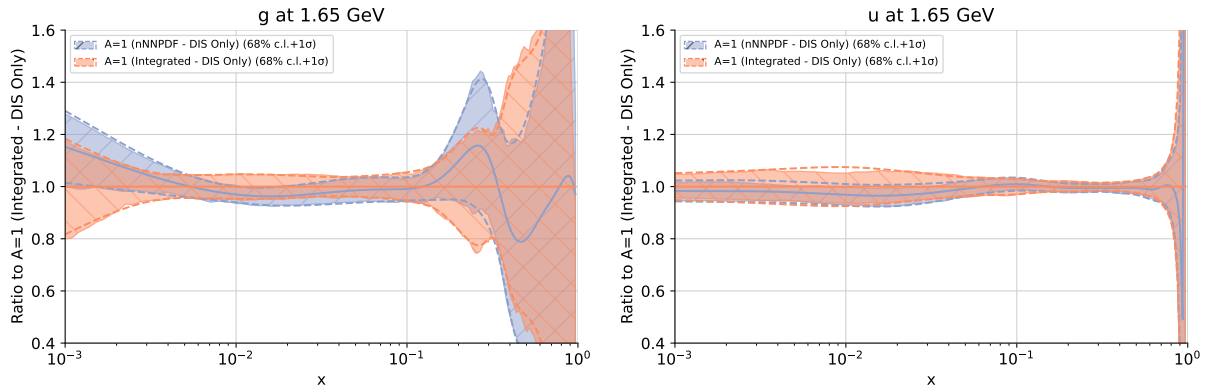


Figure 4: Comparison of the free-proton PDFs determined using the default NNPDF4.0 methodology and the integrated methodology in which the nuclear PDFs are also determined simultaneously. Solid and dashed bands correspond to 68% c.l. and one-sigma uncertainties, respectively.

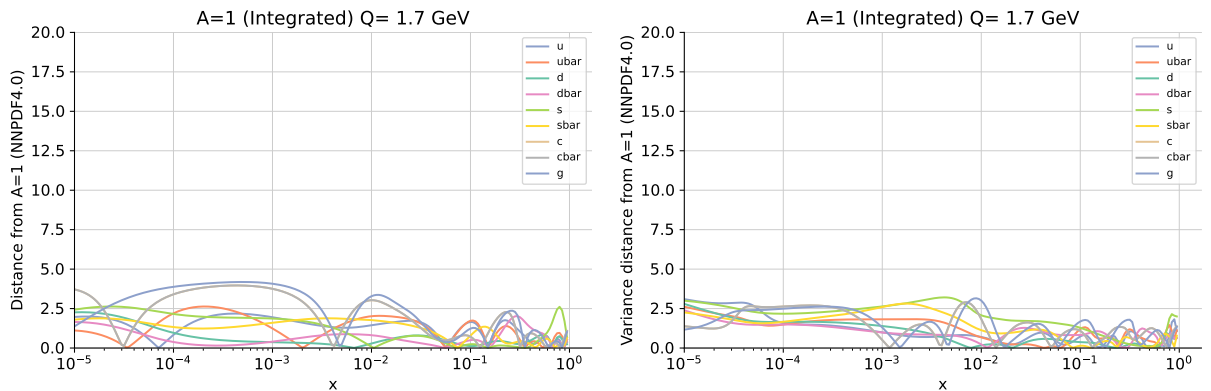


Figure 5: Distance between the central values (left) and the uncertainties (right) of the integrated free-proton PDF determination w.r.t the proton PDF determined using the NNPDF4.0 methodology. The results are shown for all PDF flavors at $Q^2 = 1.7 \text{ GeV}^2$.

only fit. This might potentially be a sign of an unbalanced fit in that the integrated fit is slightly overlearning along the proton direction – which contains much more data points – while underlearning along the nuclear directions. Such an instability could be seen when looking at the distribution of the training $E_{\text{tr}}^{(k)}$ and validation $E_{\text{val}}^{(k)}$ errors evaluated over the different MC replicas as shown in Fig. 2. In general, one expects that the values of $E_{\text{tr}}^{(k)}$ are smaller than those of $E_{\text{val}}^{(k)}$, however, as opposed to the case of the free-proton fit, very few points are located below the diagonal line. This observation is further strengthened by looking at the distribution of training lengths as shown in Fig. 3 in which one can see that not only most of the replicas reached the maximum number of iterations but also exhibit a bimodal distribution. This indicates that in order to further stabilize the integrated fits, a k -folding hyperoptimization – on the combined proton, deuteron, and nuclear datasets – is necessary to find the best combinations of hyperparameters. Given that this is an exhaustive task, we henceforth, present results based on the default hyperparameters.

Towards integrated (n)PDFs. We now study the impacts of the integrated determination by comparing the resulting (n)PDFs with the proton and nuclear PDFs determined using the NNPDF4.0 and nNNPDF methodology respectively. We recall that the comparisons shown henceforth are for DIS-only fits with NNLO QCD theory and perturbative charm.

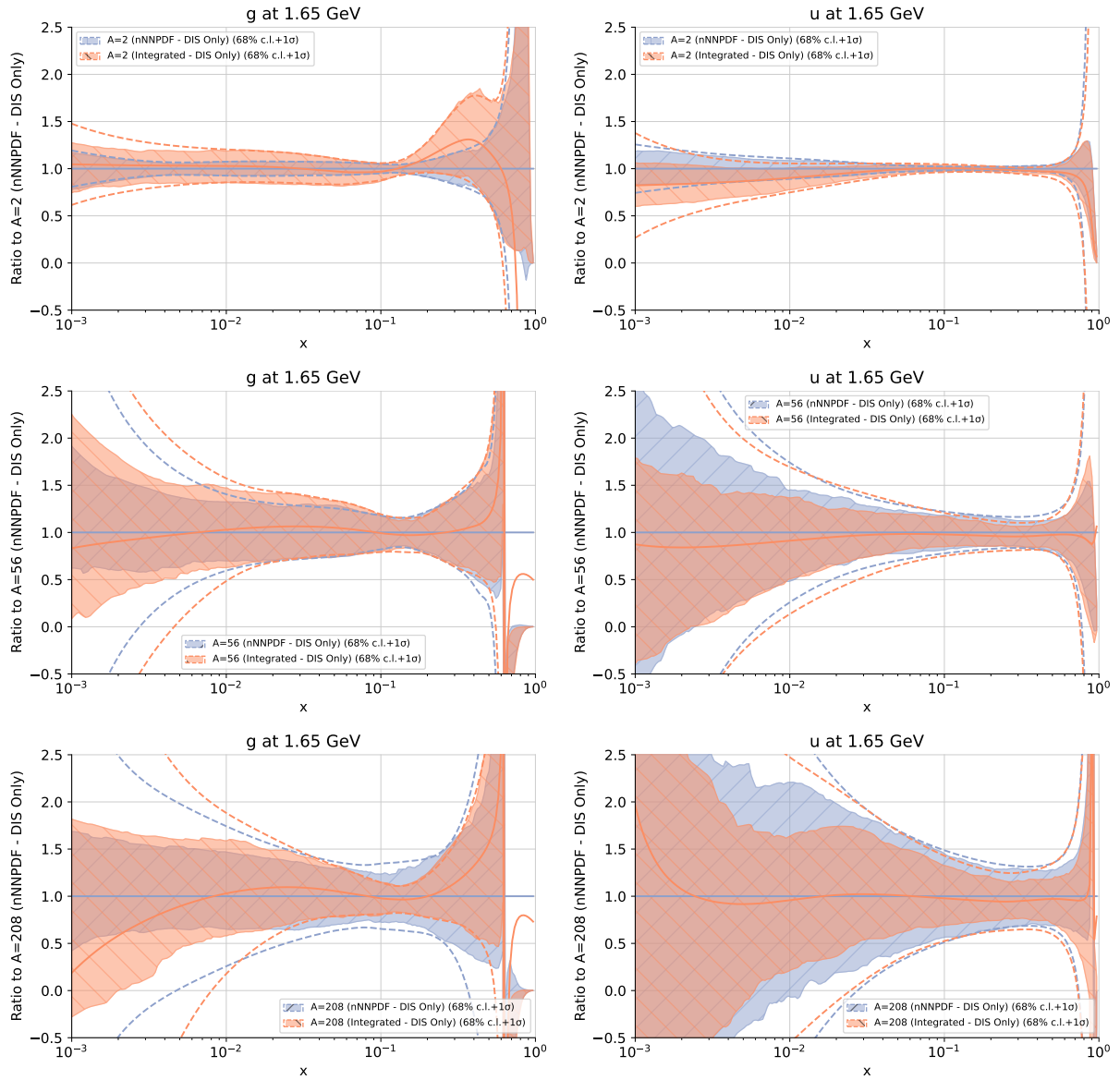


Figure 6: Comparison between the nNNPDF and integrated approaches for nuclear PDF determination. The results are shown for ${}^2\text{D}$, ${}^{56}\text{Fe}$, and ${}^{208}\text{Pb}$ for the up and gluon nPDFs at $Q^2 = 1.65 \text{ GeV}^2$. The results are normalized to the central values of the PDFs determined from the nNNPDF approach. The solid and dashed bands represent the 68% c.l. and one-sigma uncertainties, respectively.

Let us first examine the proton-PDFs determined using the integrated approach. In Fig. 4 we show the comparison of the NNPFD4.0 and integrated approaches for the up and gluon PDFs as a function of x at the fitting scale $Q_0 = 1.65 \text{ GeV}^2$. The results are normalized to the central values of the PDFs determined in the integrated approach. The solid and dashed uncertainty bands represent the 68% confidence level interval and the one-sigma error, respectively. In general, there is an excellent agreement between the proton PDFs determined using the default NNPFD4.0 methodology and the integrated approach. Marked wiggles can be observed in the integrated determination which could be connected to the slight overfitting discussed in the previous section. The consistency between the two approaches is further supported by the distance plots shown in Fig. 5. Displayed are the absolute and variance distance measured from the default NNPFD4.0 determination on the flavor basis as a function of x at $Q^2 = 1.7 \text{ GeV}^2$. As we can see, the differences in both the central values and uncertainties are well within one sigma.

We now turn to the comparisons of the deuteron and heavier nuclear PDFs. Fig. 6 displays the comparisons between the nNNPDF and integrated approaches for the deuteron (^2D), and two heavier nuclei – namely Iron (^{56}Fe) and lead (^{208}Pb). The results are shown as a function of x for the up and gluon nPDFs at $Q^2 = 1.65 \text{ GeV}^2$. Similar to the previous results, the solid and dashed bands represent the 68% c.l. and one-sigma uncertainties, respectively. All results are normalized to the central values of the integrated nPDFs. The two determinations are overall in excellent agreement within the uncertainties although in general the nPDFs determined using the integrated approach yield larger uncertainties and more fluctuations. This can be markedly seen for instance for the gluon PDF of the deuteron. More pronounced differences are observed for both the up and gluon PDF of the lead in which the integrated method yield much smaller error at medium- and large- x .

These comparisons demonstrate that albeit the issues regarding the stability of the integrated fit – which is directly linked to the choice of hyperparameters – the framework is working and is capable of reproducing the reference fits in which the proton and nuclear PDFs are separately determined.

Conclusions and outlook. We presented a framework in which the proton, deuteron, and heavy nuclear parton distributions are simultaneously determined without the need for imposing a boundary condition to reproduce the $A = 1$ limit. It is based on the integration of the framework underpinning the nNNPDF3.0 determination of the parton distribution of nucleons bound within nuclei into that adopted in the NNPDF4.0 methodology for the determination of free-proton PDFs.

It was shown that the (n)PDFs extracted from the integrated approach are consistent with the reference (n)NNPDF determinations. However, using the default NNPDF4.0 set of hyperparameters did not yield desirable results due to the sign of instability in the training. After all, the underlying nature of the neural network architecture has drastically changed due to the additional parametrization of the atomic mass number A . Therefore, a k -folding-based scan of the parameter space must be performed in order to obtain the best combination of hyperparameters.

From the physics’ point of view, in order to achieve a reliable separation between quark flavors, we must extend the experimental datasets to include hadronic processes. All the ingredients should be indeed available to perform a global nuclear PDF fit with NNLO QCD calculations with fitted charm. Once this is done, the next steps will be to include estimation of missing higher order uncertainties [18–20], and to provide an approximate N3LO (n)PDF integrated determination [21, 22].

Acknowledgments. The author is grateful to Juan Rojo for the careful reading of the manuscript. The author also wishes to thank the collaborators from the Netherlands eScience Center (NLeSC) for discussions during the development of the project. This work is supported by an Accelerating Scientific Discoveries grant of the NLeSC.

References

- [1] R. Abdul Khalek et al., *Snowmass 2021 White Paper: Electron Ion Collider for High Energy Physics*, [arXiv:2203.13199](https://arxiv.org/abs/2203.13199).
- [2] R. Abdul Khalek et al., *Science Requirements and Detector Concepts for the Electron-Ion Collider: EIC Yellow Report*, *Nucl. Phys. A* **1026** (2022) 122447, [[arXiv:2103.05419](https://arxiv.org/abs/2103.05419)].

- [3] P. Azzi et al., *Report from Working Group 1: Standard Model Physics at the HL-LHC and HE-LHC*, *CERN Yellow Rep. Monogr.* **7** (2019) 1–220, [[arXiv:1902.04070](#)].
- [4] J. J. Ethier and E. R. Nocera, *Parton Distributions in Nucleons and Nuclei*, *Ann. Rev. Nucl. Part. Sci.* **70** (2020) 43–76, [[arXiv:2001.07722](#)].
- [5] R. D. Ball, A. Candido, S. Forte, F. Hekhorn, E. R. Nocera, J. Rojo, and C. Schwan, *Parton distributions and new physics searches: the Drell–Yan forward–backward asymmetry as a case study*, *Eur. Phys. J. C* **82** (2022), no. 12 1160, [[arXiv:2209.08115](#)].
- [6] **NNPDF** Collaboration, R. D. Ball et al., *The path to proton structure at 1% accuracy*, *Eur. Phys. J. C* **82** (2022), no. 5 428, [[arXiv:2109.02653](#)].
- [7] **NNPDF** Collaboration, R. D. Ball et al., *An open-source machine learning framework for global analyses of parton distributions*, *Eur. Phys. J. C* **81** (2021), no. 10 958, [[arXiv:2109.02671](#)].
- [8] R. D. Ball and A. Deshpande, *The proton spin, semi-inclusive processes, and measurements at a future Electron Ion Collider*, pp. 205–226. 2019. [[arXiv:1801.04842](#)].
- [9] **NNPDF** Collaboration, R. D. Ball, E. R. Nocera, and R. L. Pearson, *Nuclear Uncertainties in the Determination of Proton PDFs*, *Eur. Phys. J. C* **79** (2019), no. 3 282, [[arXiv:1812.09074](#)].
- [10] R. D. Ball, E. R. Nocera, and R. L. Pearson, *Deuteron Uncertainties in the Determination of Proton PDFs*, *Eur. Phys. J. C* **81** (2021), no. 1 37, [[arXiv:2011.00009](#)].
- [11] **NNPDF** Collaboration, R. Abdul Khalek, J. J. Ethier, and J. Rojo, *Nuclear parton distributions from lepton-nucleus scattering and the impact of an electron-ion collider*, *Eur. Phys. J. C* **79** (2019), no. 6 471, [[arXiv:1904.00018](#)].
- [12] R. Abdul Khalek, J. J. Ethier, J. Rojo, and G. van Weelden, *nNNPDF2.0: quark flavor separation in nuclei from LHC data*, *JHEP* **09** (2020) 183, [[arXiv:2006.14629](#)].
- [13] R. Abdul Khalek, R. Gauld, T. Giani, E. R. Nocera, T. R. Rabemananjara, and J. Rojo, *nNNPDF3.0: evidence for a modified partonic structure in heavy nuclei*, *Eur. Phys. J. C* **82** (2022), no. 6 507, [[arXiv:2201.12363](#)].
- [14] R. A. Khalek, J. J. Ethier, E. R. Nocera, and J. Rojo, *Self-consistent determination of proton and nuclear PDFs at the Electron Ion Collider*, *Phys. Rev. D* **103** (2021), no. 9 096005, [[arXiv:2102.00018](#)].
- [15] **Jefferson Lab Angular Momentum (JAM)** Collaboration, E. Moffat, W. Melnitchouk, T. C. Rogers, and N. Sato, *Simultaneous Monte Carlo analysis of parton densities and fragmentation functions*, *Phys. Rev. D* **104** (2021), no. 1 016015, [[arXiv:2101.04664](#)].
- [16] A. Barontini, A. Candido, J. M. Cruz-Martinez, F. Hekhorn, and C. Schwan, *Pineline: Industrialization of High-Energy Theory Predictions*, [[arXiv:2302.12124](#)].

- [17] A. Candido, A. Garcia, G. Magni, T. Rabemananjara, J. Rojo, and R. Stegeman, *Neutrino Structure Functions from GeV to EeV Energies*, *JHEP* **05** (2023) 149, [[arXiv:2302.08527](#)].
- [18] **NNPDF** Collaboration, R. Abdul Khalek et al., *A first determination of parton distributions with theoretical uncertainties*, *Eur. Phys. J. C* (2019) 79:838, [[arXiv:1905.04311](#)].
- [19] **NNPDF** Collaboration, R. Abdul Khalek et al., *Parton Distributions with Theory Uncertainties: General Formalism and First Phenomenological Studies*, *Eur. Phys. J. C* **79** (2019), no. 11 931, [[arXiv:1906.10698](#)].
- [20] R. D. Ball and R. L. Pearson, *Correlation of theoretical uncertainties in PDF fits and theoretical uncertainties in predictions*, *Eur. Phys. J. C* **81** (2021), no. 9 830, [[arXiv:2105.05114](#)].
- [21] F. Hekhorn and G. Magni, *DGLAP evolution of parton distributions at approximate N^3LO* , [arXiv:2306.15294](#).
- [22] J. McGowan, T. Cridge, L. A. Harland-Lang, and R. S. Thorne, *Approximate N^3LO parton distribution functions with theoretical uncertainties: MSHT20a N^3LO PDFs*, *Eur. Phys. J. C* **83** (2023), no. 3 185, [[arXiv:2207.04739](#)]. [Erratum: *Eur.Phys.J.C* 83, 302 (2023)].